Journal of Solid Mechanics Vol. 10, No. 1 (2018) pp. 130-141

Magneto-Electro-Thermo-Mechanical Response of a Multiferroic Doubly-Curved Nano-Shell

S. Razavi *

Young Researchers and Elite Club, Tabriz Branch, Islamic Azad University, Tabriz, Iran

Received 9 November 2017; accepted 7 January 2018

ABSTRACT

Free vibration of a simply-supported magneto-electro-elastic doubly-curved nano-shell is studied based on the first-order shear deformation theory in the presence of the rotary inertia effect. To model the electric and magnetic behaviors of the nano-shell, Gauss's laws for electrostatics and magneto statics are used. By using Navier's method, the partial differential equations of motion are reduced to a single ordinary differential equation. Then, an analytical relation is obtained for the natural frequency of magneto-electro-elastic doubly-curved nano-shell. Some examples are presented to validate the proposed model. Moreover, the effects of the electric and magnetic potentials, temperature rise, nonlocal parameter, parameters of Pasternak foundation, and the geometry of the nano-shell on the natural frequencies of magneto-electro-elastic doubly-curved nano-shells are investigated. It is found that natural frequency of magneto-electro-elastic doubly-curved nano-shell decreases with increasing the temperature, increasing the electric potential, or decreasing the magnetic potential.

Keywords: Magneto-electro-elastic; Nano-shell; Doubly-curved; First-order theory.

1 INTRODUCTION

MAGNETO-ELECTRO-ELASTIC (MME) materials are smart materials exhibiting magneto-electric (ME) coupling which enables them to convert mechanical, electrical and magnetic energies to each other. Understanding the vibration behavior of nano-structures is the key step in designing nano-sized devices like sensors. So, it is important to study the vibration response of MEE nano-structures before using them as sensors, actuators, energy harvesters, etc.

Arash and Wang [1] introduced and reviewed several nonlocal continuum models to model carbon nano-tubes and graphene sheets. Pradhan and Kumar [2] and Babaei and Shahidi [3], respectively, used differential quadrature (DQ) and Galerkin methods to determine the vibration response of graphene sheets. Three-dimensional (3D) theory [4], Mindlin plate theory [5], higher-order shear deformation theory (HSDT) [6], and refined plate theory (RPT) [7] in conjunction with nonlocal continuum theory are used to study the vibration behavior of nano-plates. Analooei et al. [8] used finite strip method to study the vibration of isotropic and orthotropic nano-plates. Aksencer and Aydogdu [9] used Navier-type solution for vibration analysis of simply-supported nano-plate. They also used Levy-type solution for vibration analysis of nano-plates with two opposite edges simply-supported and the others

*Corresponding author. Tel.: +98 914 1051582.
E-mail address: soheilrazavi@outlook.com (S.Razavi).

arbitrary. Tadi Beni et al. [10] and Rouhi et al. [11] presented shear deformable models for free vibration analysis of cylindrical nano-shells. Pouresmaeeli et al. [12] studied the vibration behavior of simply-supported viscoelastic nano-plate based on nonlocal Kirchhoff theory. They found that the frequency decreases with increasing the structural damping coefficient. Ghorbanpour Arani et al. [13] studied the free vibration of a magnetostrictive nano-plate based on Reddy's third-order shear deformation theory (TSDT) and Eringen's nonlocal continuum model. Vibration of nano-tube reinforced fluid-conveying micro-tubes supported by visco-Pasternak foundation has also been investigated by Arani et al. [14]. Liu et al. [15] and Ke et al. [16] investigated vibration of piezoelectric nano-plates based on nonlocal Kirchhoff and nonlocal Mindlin theories, respectively. Ke et al. [17] studied thermo-electro-mechanical vibration of piezoelectric cylindrical nano-shells using nonlocal Love's thin shell theory. Vaezi et al. [18] investigated the effects of electric and magnetic potentials on the free vibration of a MEE micro-beam based on Euler-Bernoulli beam theory. Amiri et al. [19] used a MEE beam model to study the vibration and instability of fluid conveying smart micro-tubes. Ebrahimi and Barati [20] examined vibrational behavior of a magneto-electro-viscoelastic nano-beam based on HSDT. Li et al. [21] studied the bending, buckling and free vibration of MEE nano-beams based on nonlocal Timoshenko theory. They determined the effects of electric and magnetic potentials on the vibration response of these nano-beams. Nonlocal TSDT [22] and nonlocal Timoshenko theory [23] have been used by Ansari et al. to study the nonlinear forced vibration of a MEE nano-beam. Ke and Wang [24] used nonlocal Timoshenko theory in conjunction with DQ method to obtain the free vibration response of a MEE nano-beam. Ke et al. [25] studied the free vibration of a MEE nano-plate based on the nonlocal Kirchhoff plate. They found that the natural frequency of the MEE nano-plate is sensitive to mechanical, electrical and magnetic loadings, while it is insensitive to the thermal loading. By considering surface and nonlocal effects, Wang et al. [26] introduced a two-dimensional theory to study the response of MEE nano-plates. Li et al. [27] investigated buckling and free vibration of a MEE nano-plate resting on Pasternak foundation based on nonlocal Mindlin theory. Pan and Waksmanski [28] presented exact closed-form solution for the 3D deformation of a layered MEE plate with nonlocal effect. Ansari and Gholami [29] studied the free vibration of MEE nano-plates in pre- and post-buckled states based on nonlocal Mindlin theory in conjunction with pseudo-arc length continuation approach. Farajpour et al. [30] used nonlocal Kirchhoff theory in conjunction with a perturbation method to obtain closed-form expression for nonlinear frequency of a MEE nano-plate with movable and immovable simply-supported boundary conditions. Ke et al. [31] presented a model based on nonlocal Love's shell theory to investigate the vibration response of a MEE cylindrical nano-shell. Ghadiri and Safarpour [32] investigated the free vibration response of MEE cylindrical nano-shells based on first-order shear deformation theory (FSDT) and Navier-type method. Mohammadimehr et al. [33] studied the free vibration of MEE cylindrical panels reinforced by carbon nano-tubes.

To the best of the author's knowledge, the free vibration of MEE doubly-curved nano-shells has not been studied. So, free vibration of a simply-supported magneto-electro-elastic doubly-curved nano-shell is studied based on FSDT and Gauss's laws for electrostatics and magneto statics. After obtaining a closed-form relation for the natural frequency, some examples are presented to validate the proposed method. Finally, the effects of several parameters on the natural frequencies of MEE doubly-curved nano-shells are investigated.

2 PROBLEM MODELING

Based on FSDT, the displacement field of a shallow doubly-curved shell is expressed by [34]:

$$u = u_0 + z\,\theta_x, \quad v = v_0 + z\,\theta_y, \quad w = w_0 \tag{1}$$

where u_0, v_0, and w_0 are the displacements of the mid-surface along x, y, and z directions, respectively, and θ_x and θ_y are the rotations of a transverse normal about the y and x directions, respectively. Using this displacement field, one can obtain the strain–displacement relations [34]:

$$\varepsilon_x = u_{0,x} + w_0/R_x + z\,\theta_{x,x}, \quad \varepsilon_y = v_{0,y} + w_0/R_y + z\,\theta_{y,y} \tag{2}$$

$$\gamma_{yz} = w_{0,y} + \theta_y, \quad \gamma_{xz} = w_{0,x} + \theta_x, \quad \gamma_{xy} = u_{0,y} + v_{0,x} + z\left(\theta_{x,y} + \theta_{y,x}\right) \tag{3}$$

For a transversely-isotropic MEE nano-material, the constitutive relations can be written as [27]:

$$\left(1-\eta\nabla^2\right)\begin{Bmatrix}\sigma_x\\ \sigma_y\\ \tau_{yz}\\ \tau_{xz}\\ \tau_{xy}\end{Bmatrix}=\begin{bmatrix}C_{11} & C_{12} & 0 & 0 & 0\\ C_{12} & C_{22} & 0 & 0 & 0\\ 0 & 0 & C_{44} & 0 & 0\\ 0 & 0 & 0 & C_{55} & 0\\ 0 & 0 & 0 & 0 & C_{66}\end{bmatrix}\begin{Bmatrix}\varepsilon_x\\ \varepsilon_y\\ \gamma_{yz}\\ \gamma_{xz}\\ \gamma_{xy}\end{Bmatrix}+\begin{bmatrix}0 & 0 & e_{31}\\ 0 & 0 & e_{32}\\ 0 & e_{24} & 0\\ e_{15} & 0 & 0\\ 0 & 0 & 0\end{bmatrix}\begin{Bmatrix}0\\ 0\\ \phi_{,z}\end{Bmatrix}+\begin{bmatrix}0 & 0 & q_{31}\\ 0 & 0 & q_{32}\\ 0 & q_{24} & 0\\ q_{15} & 0 & 0\\ 0 & 0 & 0\end{bmatrix}\begin{Bmatrix}0\\ 0\\ \psi_{,z}\end{Bmatrix}-\begin{Bmatrix}\beta_{11}\\ \beta_{22}\\ 0\\ 0\\ 0\end{Bmatrix}\Delta T \tag{4}$$

$$\left(1-\eta\nabla^2\right)\begin{Bmatrix}D_x\\ D_y\\ D_z\end{Bmatrix}=\begin{bmatrix}0 & 0 & 0 & e_{15} & 0\\ 0 & 0 & e_{24} & 0 & 0\\ e_{31} & e_{32} & 0 & 0 & 0\end{bmatrix}\begin{Bmatrix}\varepsilon_x\\ \varepsilon_y\\ \gamma_{yz}\\ \gamma_{xz}\\ \gamma_{xy}\end{Bmatrix}-\begin{bmatrix}\eta_{11} & 0 & 0\\ 0 & \eta_{22} & 0\\ 0 & 0 & \eta_{33}\end{bmatrix}\begin{Bmatrix}0\\ 0\\ \phi_{,z}\end{Bmatrix}-\begin{bmatrix}d_{11} & 0 & 0\\ 0 & d_{22} & 0\\ 0 & 0 & d_{33}\end{bmatrix}\begin{Bmatrix}0\\ 0\\ \psi_{,z}\end{Bmatrix}+\begin{Bmatrix}0\\ 0\\ p_z\end{Bmatrix}\Delta T \tag{5}$$

$$\left(1-\eta\nabla^2\right)\begin{Bmatrix}B_x\\ B_y\\ B_z\end{Bmatrix}=\begin{bmatrix}0 & 0 & 0 & q_{15} & 0\\ 0 & 0 & q_{24} & 0 & 0\\ q_{31} & q_{32} & 0 & 0 & 0\end{bmatrix}\begin{Bmatrix}\varepsilon_x\\ \varepsilon_y\\ \gamma_{yz}\\ \gamma_{xz}\\ \gamma_{xy}\end{Bmatrix}-\begin{bmatrix}d_{11} & 0 & 0\\ 0 & d_{22} & 0\\ 0 & 0 & d_{33}\end{bmatrix}\begin{Bmatrix}0\\ 0\\ \phi_{,z}\end{Bmatrix}-\begin{bmatrix}\mu_{11} & 0 & 0\\ 0 & \mu_{22} & 0\\ 0 & 0 & \mu_{33}\end{bmatrix}\begin{Bmatrix}0\\ 0\\ \psi_{,z}\end{Bmatrix}+\begin{Bmatrix}0\\ 0\\ m_z\end{Bmatrix}\Delta T \tag{6}$$

where $\{\boldsymbol{\sigma}\}$ and $\{\boldsymbol{\varepsilon}\}$ are stress and strain vectors, respectively; $\{\boldsymbol{D}\}$ and $\{\boldsymbol{B}\}$ are the electric displacement and magnetic flux density vectors, respectively; $\{\boldsymbol{E}\} = \{0 \quad 0 \quad -\phi_{,z}\}^T$ and $\{\boldsymbol{H}\} = \{0 \quad 0 \quad -\psi_{,z}\}^T$ are electric field and magnetic field vectors, respectively, where ϕ and ψ denote electric and magnetic potentials; $[C_{ij}]$, $[\eta_{ij}]$ and $[\mu_{ij}]$ are the elastic, dielectric and magnetic permeability coefficient matrices, respectively; $[e_{ij}]$, $[q_{ij}]$ and $[d_{ij}]$ are the piezoelectric, piezo magnetic, and ME coefficient matrices, respectively; p_z, m_z and β_{ii} are pyroelectric, pyro magnetic and thermal moduli, respectively; ΔT denotes the temperature change, ∇^2 is the Laplace operator, and η is the nonlocal parameter revealing the size effect on the response of the nano-shell.

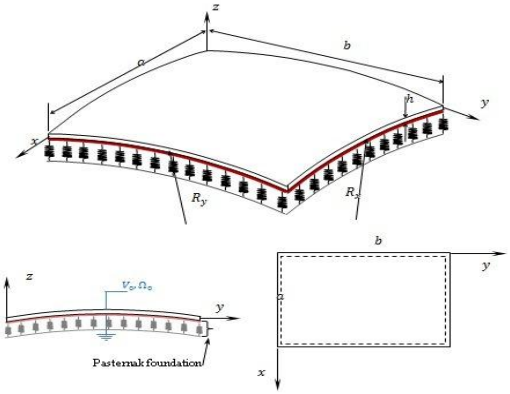

Fig.1
Schematic of the studied nano-shell.

Using Hamilton's principle and based on FSDT, the equations of motion of the nano-shell resting on a Pasternak foundation (Fig.1) can be expressed by [34]:

$$N_{x,x}+N_{xy,y}=0 \tag{7}$$

$$N_{xy,x}+N_{y,y}=0 \tag{8}$$

$$Q_{x,x}+Q_{y,y}+\left(N_x w_{0,x}+N_{xy}w_{0,y}\right)_{,x}+\left(N_{xy}w_{0,x}+N_y w_{0,y}\right)_{,y}-\frac{N_x}{R_x}-\frac{N_y}{R_y}-k_w w_0+k_s\nabla^2 w_0=I_0 w_{0,tt} \tag{9}$$

$$M_{x,x} + M_{xy,y} - Q_x = I_2 \theta_{x,tt} \tag{10}$$

$$M_{xy,x} + M_{y,y} - Q_y = I_2 \theta_{y,tt} \tag{11}$$

where $\{N_x \quad N_y \quad N_{xy}\} = \int_{-h/2}^{h/2} \{\sigma_x \quad \sigma_y \quad \sigma_{xy}\} dz$ are the in-plane force resultants, $\{Q_x \quad Q_y\} = K \int_{-h/2}^{h/2} \{\sigma_{xz} \quad \sigma_{yz}\} dz$ are the transverse force resultants, $\{M_x \quad M_y \quad M_{xy}\} = \int_{-h/2}^{h/2} \{\sigma_x \quad \sigma_y \quad \sigma_{xy}\} z dz$ are the moments resultants, and $\{I_0 \quad I_2\} = \int_{-h/2}^{h/2} \{1 \quad z^2\} \rho_0 dz$ are the mass moments of inertia, in which ρ_0 is the material density and K is the shear correction factor. Moreover, k_w and k_s are spring and shear coefficients of the Pasternak foundation, respectively. To determine theses resultants, the stress components given in Eq. (4) must be used. However, potentials ϕ and ψ are unknown parameters. To determine them, Gauss' laws for electrostatics and magneto statics are used:

$$D_{x,x} + D_{y,y} + D_{z,z} = 0 \qquad B_{x,x} + B_{y,y} + B_{z,z} = 0 \tag{12}$$

Then, using Eqs. (5), (6) and (12) gives:

$$\phi_{,z} = \phi_1 z + \phi_0 \tag{13}$$

$$\psi_{,z} = \psi_1 z + \psi_0 \tag{14}$$

where ϕ_0 and ψ_0 are constants of integration, and ϕ_1 and ψ_1 are obtained by:

$$\begin{aligned}
\phi_1 = \frac{1}{d_{33}^2 - \mu_{33}\eta_{33}} \{ & (d_{33}q_{15} - \mu_{33}e_{15}) w_{0,xx} + (d_{33}q_{24} - \mu_{33}e_{24}) w_{0,yy} + \left[d_{33}(q_{15} + q_{31}) - \mu_{33}(e_{15} + e_{31}) \right] \theta_{x,x} + \\
& \left[d_{33}(q_{24} + q_{31}) - \mu_{33}(e_{24} + e_{31}) \right] \theta_{y,y} \} \\
\psi_1 = \frac{1}{d_{33}^2 - \mu_{33}\eta_{33}} \{ & (d_{33}e_{15} - \eta_{33}q_{15}) w_{0,xx} + (d_{33}e_{24} - \eta_{33}q_{24}) w_{0,yy} + \left[d_{33}(e_{15} + e_{31}) - \eta_{33}(q_{15} + q_{31}) \right] \theta_{x,x} + \\
& \left[d_{33}(e_{24} + e_{31}) - \eta_{33}(q_{24} + q_{31}) \right] \theta_{y,y} \}
\end{aligned} \tag{15}$$

To determine ϕ_0 and ψ_0, the ME boundary condition on top and bottom surfaces of the nano-shell is needed. If the nano-shell is poled along the z direction and subjected to electric potential V_0 and magnetic potential Ω_0 between the upper and lower surfaces, the ME boundary condition can be expressed as below:

$$\begin{aligned}
& \phi\left(x, y, z = -\frac{h}{2}\right) = 0, \quad \phi\left(x, y, z = +\frac{h}{2}\right) = V_0 \\
& \psi\left(x, y, z = -\frac{h}{2}\right) = 0, \quad \psi\left(x, y, z = +\frac{h}{2}\right) = \Omega_0
\end{aligned} \tag{16}$$

Eqs. (13) – (16) yield $\phi_0 = V_0/h$ and $\psi_0 = \Omega_0/h$. Then, the resultants are obtained:

$$\left(1 - \eta\nabla^2\right) N_x = C_{11} h u_{0,x} + C_{12} h v_{0,y} + \left(\frac{C_{11}}{R_x} + \frac{C_{12}}{R_y} \right) h w_0 + e_{31} V_0 + q_{31} \Omega_0 - \beta_{11} h \Delta T \tag{17}$$

$$\left(1 - \eta\nabla^2\right) N_y = C_{12} h u_{0,x} + C_{22} h v_{0,y} + \left(\frac{C_{12}}{R_x} + \frac{C_{22}}{R_y} \right) h w_0 + e_{32} V_0 + q_{32} \Omega_0 - \beta_{22} h \Delta T \tag{18}$$

$$\left(1-\eta\nabla^2\right)N_{xy} = C_{66}h\left(u_{0,y}+v_{0,x}\right) \tag{19}$$

$$\left(1-\eta\nabla^2\right)M_x = M_1 w_{0,xx}+M_2 w_{0,yy}+M_3\theta_{x,x}+M_4\theta_{y,y} \tag{20}$$

$$\left(1-\eta\nabla^2\right)M_y = M_1 w_{0,xx}+M_2 w_{0,yy}+M_5\theta_{x,x}+M_6\theta_{y,y} \tag{21}$$

$$\left(1-\eta\nabla^2\right)M_{xy} = \frac{h^3}{12}C_{66}\left(\theta_{x,y}+\theta_{y,x}\right) \tag{22}$$

$$\left(1-\eta\nabla^2\right)Q_x = KhC_{55}\left(w_{0,x}+\theta_x\right) \tag{23}$$

$$\left(1-\eta\nabla^2\right)Q_y = KhC_{44}\left(w_{0,y}+\theta_y\right) \tag{24}$$

where

$$\begin{aligned}
M_1 &= \frac{e_{31}h^3\left(d_{33}q_{15}-\mu_{33}e_{15}\right)}{12\left(d_{33}^2-\mu_{33}\eta_{33}\right)}+\frac{q_{31}h^3\left(d_{33}e_{15}-\eta_{33}q_{15}\right)}{12\left(d_{33}^2-\mu_{33}\eta_{33}\right)}\\
M_2 &= \frac{e_{31}h^3\left(d_{33}q_{24}-\mu_{33}e_{24}\right)}{12\left(d_{33}^2-\mu_{33}\eta_{33}\right)}+\frac{q_{31}h^3\left(d_{33}e_{24}-\eta_{33}q_{24}\right)}{12\left(d_{33}^2-\mu_{33}\eta_{33}\right)}\\
M_3 &= \frac{h^3}{12}C_{11}+\frac{e_{31}h^3\left[d_{33}\left(q_{15}+q_{31}\right)-\mu_{33}\left(e_{15}+e_{31}\right)\right]}{12\left(d_{33}^2-\mu_{33}\eta_{33}\right)}+\frac{q_{31}h^3\left[d_{33}\left(e_{15}+e_{31}\right)-\eta_{33}\left(q_{15}+q_{31}\right)\right]}{12\left(d_{33}^2-\mu_{33}\eta_{33}\right)}\\
M_4 &= \frac{h^3}{12}C_{12}+\frac{e_{31}h^3\left[d_{33}\left(q_{24}+q_{31}\right)-\mu_{33}\left(e_{24}+e_{31}\right)\right]}{12\left(d_{33}^2-\mu_{33}\eta_{33}\right)}+\frac{q_{31}h^3\left[d_{33}\left(e_{24}+e_{31}\right)-\eta_{33}\left(q_{24}+q_{31}\right)\right]}{12\left(d_{33}^2-\mu_{33}\eta_{33}\right)}\\
M_5 &= M_3-\frac{h^3}{12}C_{11}+\frac{h^3}{12}C_{12} \qquad\qquad M_6 = M_4-\frac{h^3}{12}C_{12}+\frac{h^3}{12}C_{22}
\end{aligned} \tag{25}$$

Substituting Eqs. (17) – (24) into Eqs. (7) – (10), and then by using

$$\begin{aligned}
u_0 &= \sum_{n=1}^{\infty}\sum_{m=1}^{\infty}U_{mn}(t)\cos\left(m\pi x/a\right)\sin\left(n\pi y/b\right)\\
v_0 &= \sum_{n=1}^{\infty}\sum_{m=1}^{\infty}V_{mn}(t)\sin\left(m\pi x/a\right)\cos\left(n\pi y/b\right)\\
w_0 &= \sum_{n=1}^{\infty}\sum_{m=1}^{\infty}W_{mn}(t)\sin\left(m\pi x/a\right)\sin\left(n\pi y/b\right)\\
\theta_x &= \sum_{n=1}^{\infty}\sum_{m=1}^{\infty}X_{mn}(t)\cos\left(m\pi x/a\right)\sin\left(n\pi y/b\right)\\
\theta_y &= \sum_{n=1}^{\infty}\sum_{m=1}^{\infty}Y_{mn}(t)\sin\left(m\pi x/a\right)\cos\left(n\pi y/b\right)
\end{aligned} \tag{26}$$

The following ordinary differential equations are obtained:

$$L_1 U + L_2 V + L_3 W = 0 \tag{27}$$

$$L_4 U + L_5 V + L_6 W = 0 \tag{28}$$

$$L_7 \ddot{W} + L_8 W + L_9 U + L_{10} V + L_{11} X + L_{12} Y + L_{13} = 0 \tag{29}$$

$$L_{14} \ddot{X} + L_{15} X + L_{16} Y + L_{17} W = 0 \tag{30}$$

$$L_{18} \ddot{Y} + L_{19} Y + L_{20} X + L_{21} W = 0 \tag{31}$$

where U, V, W, X and Y are unknown functions and (m,n) denotes the mode of vibration. In Eqs. (27) – (31) the subscript '$_{mn}$' has been dropped for brevity.

Eqs. (27) and (28) give U and V in terms of W, while Eqs. (30) and (31) give X and Y:

$$U = \frac{L_3 L_5 - L_2 L_6}{L_2 L_4 - L_1 L_5} W, \qquad V = \frac{L_1 L_6 - L_3 L_4}{L_2 L_4 - L_1 L_5} W \tag{32}$$

$$X = \frac{L_{16} L_{21} - L_2^* L_{17}}{L_1^* L_2^* - L_{16} L_{20}} W, \quad Y = \frac{L_{17} L_{20} - L_1^* L_{21}}{L_1^* L_2^* - L_{16} L_{20}} W \tag{33}$$

where $L_1^* = L_{15} + L_{14} \dfrac{d^2}{dt^2}$ and $L_2^* = L_{19} + L_{18} \dfrac{d^2}{dt^2}$ are ordinary differential operators.

Now, substituting Eqs. (32) and (33) into (29) gives:

$$M_{\text{eq}} \ddot{W} + K_{\text{eq}} W + F_s = 0 \tag{34}$$

In which M_{eq} and K_{eq} are equivalent mass and stiffness of the system and F_s is a constant parameter. These parameters are given in Appendix A. Finally, natural frequency of the nano-shell is simply determined by using $\omega_0 = \sqrt{K_{\text{eq}} / M_{\text{eq}}}$.

3 RESULTS AND DISCUSSION

In this section, first, some examples are presented to validate the proposed model. Then, the effects of several parameters on the natural frequencies of MEE doubly-curved nano-shells are investigated. The MEE nano-shell is doubly-curved and simply-supported. It is subjected to electric (V_0) and magnetic (Ω_0) potentials between its upper and bottom surfaces. For all the numerical examples the shear correction factor (K) is taken to be 5/6.

First, an isotropic spherical shell is considered and its fundamental natural frequency is obtained. The result is shown in Table 1., along with the published results based on Sanders theory (ST) [35], Donnell theory (DT) [36], HSDT [37] and 3D approach [38]. The geometric and material properties of the shell are: $a = b = 1.0118$, $h = 0.0191$, $R = 1.91$, $E = 1$, $\rho_0 = 1$ and $\nu = 0.3$. It is seen that the result obtained by present model is in good agreement with previously published ones, and the discrepancy between the results of 3D method and present method is very small.

Table 1
Fundamental natural frequency ω_0 (*rad/s*) of an isotropic spherical shell.

ST [35]	DT [36]	HSDT [37]	3D [38]	Present
0.52830	0.52864	0.50223	0.52543	0.53510

As the second comparison, the frequency ratio of an isotropic nano-plate with $a = b = 10$ *nm*, $h = 0.34$ *nm*, $E = 1.06$ *TPa*, $\rho_0 = 2250$ *kg/m*^{3}, and $v = 0.25$ is obtained for different values of nonlocal parameter. The results are presented in Table 2., where frequency ratios are determined by using the following relation:

$$\text{Frequency ratio}=\frac{\text{frequency ratio calculated using nonlocal theory}}{\text{frequency ratio calculated using local theory}} \tag{35}$$

Table 2
Frequency ratios of a graphene sheet.

η (nm^2)	Method		
	Pradhan and Kumar [2]	Pouresmaeeli et al. [39]	Present study
0	1	1	1
1	0.9139	0.91386	0.91386
2	0.8468	0.84673	0.84673
3	0.7926	0.79251	0.79251

Table 3., presents the dimensionless fundamental frequencies of an isotropic nano-plate for different nonlocal parameters, and a/h and b/a ratios. The results are compared with the ones obtained by methods based on nonlocal Kirchhoff theory (CPT), FSDT, TSDT and a RPT. Again, it is seen that the proposed model predicts the frequencies with good accuracy.

Table 3
Dimensionless fundamental frequency $\omega = \omega_0 h\sqrt{\rho_0 / G}$ of an isotropic Nano plate ($v = 0.3$).

b/a	a/h	$\eta(nm^2)$	Method				
			CPT[a]	FSDT[a]	TSDT[a]	RPT [7]	Present
1	10	0	0.0963	0.0930	0.0935	0.09303	0.09371
		1	0.0800	0.0850	0.0854	0.08502	0.08564
		2	0.0816	0.0788	0.0791	0.07877	0.07935
		3	0.0763	0.0737	0.0741	0.07373	0.07427
	20	0	0.0241	0.0239	0.0239	0.02386	0.02391
		1	0.0220	0.0218	0.0218	0.02180	0.02185
		2	0.0240	0.0202	0.0202	0.02021	0.02025
		3	0.0191	0.0189	0.0189	0.01891	0.01895
2	10	0	0.0602	0.0589	0.0591	0.05888	0.05916
		1	0.0568	0.0556	0.0557	0.05555	0.05582
		2	0.0539	0.0527	0.0529	0.05274	0.05299
		3	0.0514	0.0503	0.0505	0.05031	0.05055
	20	0	0.0150	0.0150	0.0150	0.01496	0.01498
		1	0.0142	0.0141	0.0141	0.01411	0.01414
		2	0.0135	0.0134	0.0134	0.01340	0.01342
		3	0.0129	0.0128	0.0128	0.01278	0.01280

[a] reported by Malekzadeh and Shojaee [7]

Next, dimensionless fundamental frequencies of a MEE nano-plate made of piezoelectric $BaTiO_3$ and magnetostrictive $CoFe_2O_4$ are determined. The material properties of the MEE material are given in Table 4. The dimensionless fundamental frequencies are obtained by using $\omega = \omega_0 a\sqrt{I_0/(C_{11}h)}$. Table 5., presents the frequencies for different values of nonlocal parameter. In addition, the effect of temperature rise on the dimensionless fundamental frequency has been investigated and the results are presented in Table 6. As in the case for isotropic shell and nano-plate, the proposed method approximates the frequencies of MEE nano-plate with good accuracy.

Table 4
Material properties of $BiTiO_3$-$CoFe_2O_4$ composite material [29].

Properties	$BaTiO_3$-$CoFe_2O_4$
Elastic [*GPa*]	$c_{11} = c_{22} = 226$, $c_{12} = 125$, $c_{33} = 216$, $c_{44} = c_{55} = 44.2$, $c_{66} = 50.5$
Piezoelectric [C/m^2]	$e_{31} = e_{32} = -2.2$, $e_{15} = e_{24} = 5.8$
Dielectric [$\times 10^{-9}$ $C/(Vm)$]	$\eta_{33} = 6.35$
Piezo magnetic [$N/(Am)$]	$q_{31} = q_{32} = 290.1$, $q_{15} = q_{24} = 275$
Magnetoelectric [$\times 10^{-12}$ $Ns/(CV)$]	$d_{33} = 2737.5$
Magnetic [$\times 10^{-6}$ Ns^2/C^2]	$\mu_{33} = 83.5$
Thermal Moduli [$\times 10^5$ $N/(Km^2)$]	$\beta_{11} = \beta_{22} = 4.74$
Pyroelectric [$\times 10^{-6}$ C/N]	$p_z = 25$
Pyro magnetic [$\times 10^{-6}$ $N/(AmK)$]	$m_z = 5.19$
Mass density [kg/m^3]	5550

Table 5
The effect of nonlocal parameter (η) on the dimensionless fundamental frequency of a MEE nano-plate ($\Delta T = V_0 = \Omega_0 = 0$).

Method	η ($\times 10^{-16}$)					
	0	0.36	1.44	3.24	5.76	9
Ke et al. [24]	0.3698	0.3379	0.2764	0.2219	0.1813	0.1518
Ansari and Gholami [28]	0.3684	–	0.2756	–	0.1808	–
Present study	0.3717	0.3397	0.2779	0.2231	0.1823	0.1526

Table 6
The effect of the temperature rise on the dimensionless fundamental frequency of a MEE nano-plate ($\eta = 1.44\times 10^{-16}$, $V_0 = \Omega_0 = 0$).

Method	ΔT					
	0	30	60	90	120	150
Ke et al. [24]	0.2764	0.2749	0.2734	0.2719	0.2704	0.2689
Present study	0.2779	0.2766	0.2753	0.2741	0.2729	0.2716

The effect of radius of curvature (R_x) on the dimensionless fundamental frequency of nanoscale spherical and cylindrical MEE shells is investigated and the result is shown in Fig. 2. In this example, $a = b = 60$ *nm*, $h = 4$ *nm* and $\eta = 0.2$ nm^2. It is seen that for a specific R_x, the spherical shell has higher frequency which decreases with higher rate when R_x increases.

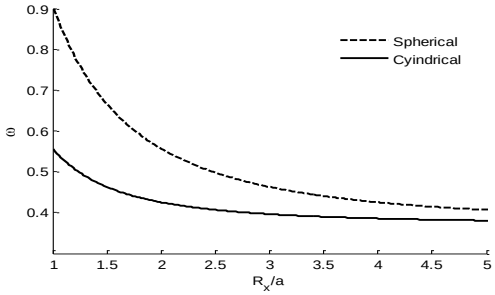

Fig.2
Dimensionless fundamental frequency of spherical and cylindrical MEE nano-shells ($\Delta T = V_0 = \Omega_0 = 0$).

Fig. 3 shows the effect of temperature change on the dimensionless fundamental frequency of two MEE nano-shells (with $a = b = 60$ *nm*, $h = 4$ *nm*, and $R = 5a$) and a MEE nano-plate (with $a = b = 60$ *nm*, $h = 4$ *nm*). For all of the structures, the dimensionless frequencies decrease with increasing the temperature.

Effects of electric and magnetic potentials on the natural frequency of MEE nano-shells are also investigated and the results are shown in Figs. 4 and 5, respectively. The geometric properties of the nano-structures are the same as previous example. It is observed that increasing the electric potential, decreases the natural frequency of MEE nano-shells. Moreover, for negative electric potentials, higher natural frequencies are resulted. The converse happens when magnetic potential changes. That is, as the magnetic potential increases, the natural frequency of the MEE nano-shell increases.

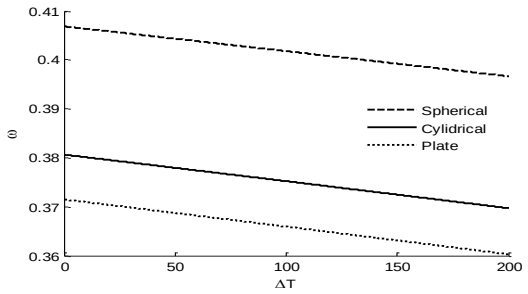

Fig.3
Effect of temperature change on the dimensionless fundamental frequency of MEE nano-structures ($\eta = 0.2\ nm^2$, $V_0 = \Omega_0 = 0$).

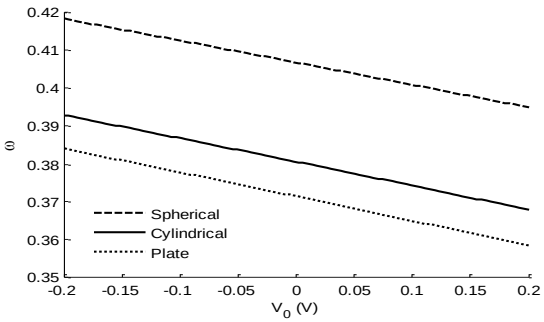

Fig.4
Effect of electric potential on the dimensionless fundamental frequency of MEE nano-structures ($\eta = 0.2\ \mathrm{nm}^2$, $\Delta T = \Omega_0 = 0$).

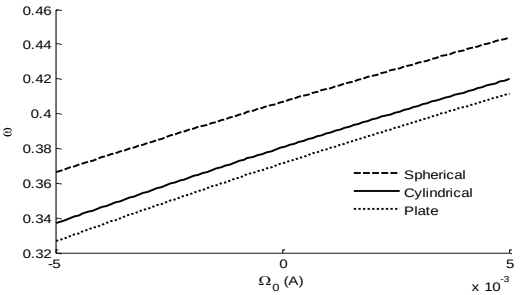

Fig.5
Effect of magnetic potential on the dimensionless fundamental frequency of MEE nano-structures ($\eta = 0.2\ \mathrm{nm}^2$, $\Delta T = V_0 = 0$).

Effects of nonlocal parameter and foundation parameters on the natural frequencies of MEE doubly-curved nano-shells are investigated, too. Fig. 6 shows the effect of nonlocal parameter on the dimensionless fundamental frequencies of spherical and cylindrical MEE nano-shells with $a = b = 60\ nm$, $h = 4\ nm$, $R = 5a$. It is seen that nonlocal parameter has small effect on the frequency and tends to decrease it. In Fig. 7, effects of foundation parameters on the dimensionless fundamental frequency of spherical MEE nano-shell with $a = b = 60\ nm$, $h = 4\ nm$, $R = 5a$ are shown. The dimensionless foundation parameters are obtained by $K_w = k_w a^4/(C_{ij\max}h^3)$ and $K_s = k_s a^2/(C_{ij\max}h^3)$ where $C_{ij\max}$ is the maximum value of the stiffness coefficients of the MEE nano-shell. It is observed that both dimensionless spring and shear coefficients increase the stiffness (and subsequently the natural frequency) of the system. However, dimensionless shear coefficient (K_s) has more effect on the natural frequency of MEE nano-shells.

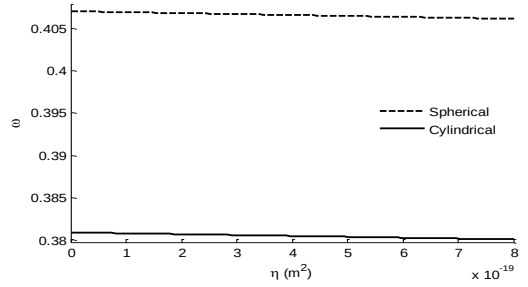

Fig.6
Variation of dimensionless fundamental frequency of MEE nano-shell in terms of nonlocal parameter ($\Delta T = V_0 = \Omega_0 = 0$).

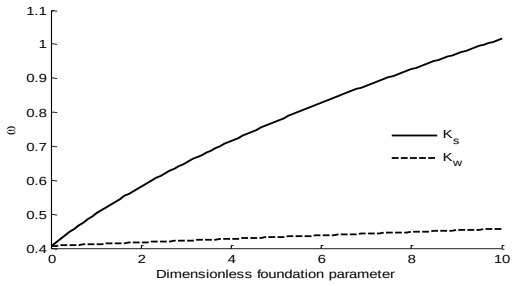

Fig.7
Variation of dimensionless fundamental frequency of spherical MEE nano-shell in terms of foundation parameters ($\eta = 0.2$ nm^2, $\Delta T = V_0 = \Omega_0 = 0$).

4 CONCLUSIONS

Free vibration of simply-supported MEE doubly-curved nano-shells is studied analytically based on FSDT. Some examples are presented and it is found that: (a) spherical nano-shell has higher natural frequencies which decrease with higher rate when the curvature of the nano-shell increases, (b) natural frequency decreases with increasing the temperature, (c) increasing the electric potential decreases the natural frequency of MEE nano-shells, (d) when the magnetic potential increases, the natural frequency of the MEE nano-shell increases, (e) nonlocal parameter decreases the natural frequency of MEE nano-shell, and (f) foundation parameters increase the natural frequencies of MEE nano-shells. However, dimensionless shear coefficient has more effect on the natural frequencies.

APPENDIX A

The coefficients of Eq. (34) are:

$$M_{\text{eq}} = \alpha_5 L_7 + \alpha_6 L_8 + \alpha_6 \left(k_1 + k_2\right) - \alpha_2 L_{11} - \alpha_4 L_{12} \tag{A.1}$$

$$K_{\text{eq}} = \alpha_5 L_8 + \alpha_5 \left(k_1 + k_2\right) + L_{11}\left(L_{16} L_{21} - \alpha_1\right) + L_{12}\left(L_{17} L_{20} - \alpha_3\right) \tag{A.2}$$

$$F_s = \alpha_{15} L_{13} \tag{A.3}$$

Where

$$\alpha_1 = L_{17} L_{19},\quad \alpha_2 = L_{17} L_{18},\quad \alpha_3 = L_{15} L_{21},\quad \alpha_1 = L_{14} L_{21},\quad \alpha_5 = L_{15} L_{19} - L_{16} L_{20},\quad \alpha_6 = L_{14} L_{19} - L_{16} L_{20} \tag{A.4}$$

$$k_1 = \frac{L_9\left(L_3 L_5 - L_2 L_6\right)}{L_2 L_4 - L_1 L_5},\qquad k_2 = \frac{L_{10}\left(L_1 L_6 - L_3 L_4\right)}{L_2 L_4 - L_1 L_5} \tag{A.5}$$

REFERENCES

[1] Arash B., Wang Q., 2012, A review on the application of nonlocal elastic models in modeling of carbon nanotubes and graphenes, *Computational Materials Science* **51**: 303-313.

[2] Pradhan S.C., Kumar A., 2010, Vibration analysis of orthotropic graphene sheets embedded in Pasternak elastic medium using nonlocal elasticity theory and differential quadrature method, *Computational Materials Science* **50**: 239-245.

[3] Babaei H., Shahidi A.R., 2013, Free vibration analysis of quadrilateral Nano plates based on nonlocal continuum models using the Galerkin method: the effects of small scale, *Meccanica* **48**(4): 971-982.

[4] Alibeigloo A., 2011, Free vibration analysis of nano-plate using three-dimensional theory of elasticity, *Acta Mechanica* **222**: 149-159.

[5] Hosseini-Hashemi S., Zare M., Nazemnezhad R., 2013, An exact analytical approach for free vibration of Mindlin rectangular nano-plates via nonlocal elasticity, *Composite Structures* **100**: 290-299.
[6] Daneshmehr A., Rajabpoor A., Hadi A., 2015, Size dependent free vibration analysis of Nano plates made of functionally graded materials based on nonlocal elasticity theory with high order theories, *International Journal of Engineering Science* **95**: 23-35.
[7] Malekzadeh P., Shojaee M., 2013, Free vibration of Nano plates based on a nonlocal two-variable refined plate theory, *Composite Structures* **95**: 443-452.
[8] Analooei H.R., Azhari M., Heidarpour A., 2013, Elastic buckling and vibration analyses of orthotropic Nano plates using nonlocal continuum mechanics and spline finite strip method, *Applied Mathematical Modelling* **37**(10-11): 6703-6717.
[9] Aksencer T., Aydogdu M., 2011, Levy type solution method for vibration and buckling of Nano plates using nonlocal elasticity theory, *Physica E* **43**: 954-959.
[10] Tadi Beni Y., Mehralian F., Razavi H., 2015, Free vibration analysis of size-dependent shear deformable functionally graded cylindrical shell on the basis of modified couple stress theory, *Composite Structures* **120**: 65-78.
[11] Rouhi H., Ansari R., Darvizeh M., 2016, Size-dependent free vibration analysis of Nano shells based on the surface stress elasticity, *Applied Mathematical Modelling* **40**: 3128-3140.
[12] Pouresmaeeli S., Ghavanloo E., Fazelzadeh S.A., 2013, Vibration analysis of viscoelastic orthotropic Nano plates resting on viscoelastic medium, *Composite Structures* **96**: 405-410.
[13] Ghorbanpour Arani A., Khoddami Maraghi Z., Khani Arani H., 2016, Orthotropic patterns of Pasternak foundation in smart vibration analysis of magnetostrictive Nano plate, *Proceedings of the Institution of Mechanical Engineers, Part C: Mechanical Engineering Science* **230**(4): 559-572.
[14] Ghorbanpour Arani A, Haghparast E, Rarani MH, Maraghi ZK, 2015, Strain gradient shell model for nonlinear vibration analysis of visco-elastically coupled Boron Nitride nano-tube reinforced composite micro-tubes conveying viscous fluid, *Computational Materials Science* **96**: 448-458.
[15] Liu C., Ke L.L., Wang Y.S., Yang J., Kitipornchai S., 2013, Thermo-electro-mechanical vibration of piezoelectric nanoplates based on the nonlocal theory, *Composite Structures* **106**: 167-174.
[16] Ke L.L., Liu C., Wang Y.S., 2015, Free vibration of nonlocal piezoelectric Nano plates under various boundary conditions, *Physica E* **66**: 93-106.
[17] Ke L.L., Wang Y.S., Reddy J.N., 2014, Thermo-electro-mechanical vibration of size-dependent piezoelectric cylindrical nanoshells under various boundary conditions, *Composite Structures* **116**: 626-636.
[18] Vaezi M., Moory Shirbany M., Hajnayeb A., 2016, Free vibration analysis of magneto-electro-elastic micro beams subjected to magneto-electric loads, *Physica E* **75**: 280-286.
[19] Amiri A., Pournaki I.J., Jafarzadeh E., Shabani R., Rezazadeh G., 2016, Vibration and instability of fluid‐conveyed smart micro‐tubes based on magneto‐electro‐elasticity beam model, *Micro Fluids Nano Fluids* **20**: 38-48.
[20] Ebrahimi F., Barati M.R., 2016, A nonlocal higher-order refined magneto-electro-viscoelastic beam model for dynamic analysis of smart nanostructures, *International Journal of Engineering Science* **107**: 183-196.
[21] Li Y.S., Ma P., Wang W., 2016, Bending, buckling, and free vibration of magnetoelectroelastic nanobeam based on nonlocal theory, *Journal of Intelligent Material Systems and Structures* **27**(9): 1139-1149.
[22] Ansari R., Hasrati E., Gholami R., Sadeghi F., 2015, Nonlinear analysis of forced vibration of nonlocal third-order shear deformable beam model of magneto-electro-thermo elastic nanobeams, *Composites Part B* **83**: 226-241.
[23] Ansari R., Gholami R., Rouhi H., 2015, Size-dependent nonlinear forced vibration analysis of magneto-electro-thermo-elastic Timoshenko Nano beams based upon the nonlocal elasticity theory, *Composite Structures* **126**: 216-226.
[24] Ke L.L., Wang Y.S., 2014, Free vibration of size-dependent magneto-electro-elastic nanobeams based on the nonlocal theory, *Physica E* **63**: 52-61.
[25] Ke L.L., Wang Y.S., Yang J., Kitipornchai S., 2014, Free vibration of size-dependent magneto-electro-elastic nanoplates based on the nonlocal theory, *Acta Mechanica Sinica* **30**(4): 516-525.
[26] Wang W., Li P., Jin F., 2016, Two-dimensional linear elasticity theory of magneto-electro-elastic plates considering surface and nonlocal effects for nanoscale device applications, *Smart Materials and Structures* **25**: 095026-095041.
[27] Li Y.S., Cai Z.Y., Shi S.Y., 2014, Buckling and free vibration of magnetoelectroelastic Nano plate based on nonlocal theory, *Composite Structures* **111**: 552-529.
[28] Pan E., Waksmanski N., 2016, Deformation of a layered magnetoelectroelastic simply-supported plate with nonlocal effect, an analytical three-dimensional solution, *Smart Materials and Structures* **25**: 095013-095030.
[29] Ansari R., Gholami R., 2016, Nonlocal free vibration in the pre- and post-buckled states of magneto-electro-thermo elastic rectangular Nano plates with various edge conditions, *Smart Materials and Structures* **25**: 095033-095050.
[30] Farajpour A., Hairi Yazdi M.R., Rastgoo A., Loghmani M., Mohammadi M., 2016, Nonlocal nonlinear plate model for large amplitude vibration of magneto-electro-elastic Nano plates, *Composite Structures* **140**: 323-336.
[31] Ke L.L., Wang Y.S., Yang J., Kitipornchai S., 2014, The size-dependent vibration of embedded magneto-electro-elastic cylindrical Nano shells, *Smart Materials and Structures* **23**: 125036-125053.
[32] Ghadiri M., Safarpour H., 2016, Free vibration analysis of embedded magneto-electro-thermo-elastic cylindrical Nano shell based on the modified couple stress theory, *Applied Physics A* **122**: 833-844.

[33] Mohammadimehr M., Okhravi S.V., Akhavan Alavi S.M., 2016, Free vibration analysis of magneto-electro-elastic cylindrical composite panel reinforced by various distributions of CNTs with considering open and closed circuits boundary conditions based on FSDT, *Journal of Vibration and Control* **24**: 1551-1569.
[34] Reddy J.N., 2004, *Mechanics of Laminated Composite Plates and Shells: Theory and Analysis*, CRC Press.
[35] Hosseini-Hashemi S., Atashipour S.R., Fadaee M., Girhammar U.A., 2012, An exact closed-form procedure for free vibration analysis of laminated spherical shell panels based on Sanders theory, *Archive of Applied Mechanics* **82**: 985-1002.
[36] Fadaee M., Atashipour S.R., Hosseini-Hashemi S., 2013, Free vibration analysis of Lévy-type functionally graded spherical shell panel using a new exact closed-form solution, *International Journal of Mechanical Sciences* **77**: 227-238.
[37] Khare R.K., Kant T., Garg A.K., 2004, Free vibration of composite and sandwich laminates with a higher-order facet shell element, *Composite Structures* **65**: 405-418.
[38] Chern Y.C., Chao C.C., 2000, Comparison of natural frequencies of laminates by 3D theory-part II: curved panels, *Journal of Sound and Vibration* **230**: 1009-1030.
[39] Pouresmaeeli S., Fazelzadeh S.A., Ghavanloo E., 2012, Exact solution for nonlocal vibration of double-orthotropic Nano plates embedded in elastic medium, *Composites Part B* **43**: 3384-3390.